Supporting information for:

Generalized Structural Description of Calcium-Sodium Aluminosilicate Hydrate gels: The Crosslinked Substituted Tobermorite Model

Rupert J. Myers [1,2], Susan A. Bernal [1,2], Rackel San Nicolas [2], John L. Provis [1,2]*

[1] Department of Materials Science and Engineering, University of Sheffield, Sheffield, UK

[2] Department of Chemical & Biomolecular Engineering, The University of Melbourne, Victoria 3010, Australia

* To whom correspondence should be addressed. Email jprovis@sheffield.ac.uk, phone +44 114 222 5490, fax +44 114 222 5943

Contents

Appendix A. Application of the CSTM to a crosslinked tobermorite

Eqs.(7-8) are applied to a crosslinked C-(N)-A-S-H with MCL = 22 to illustrate their use. The site fractions shown in Figure S1 are representative of the type of data which could be obtained by deconvolution of a ^{29}Si MAS NMR spectrum for the crosslinked C-(N)-A-S-H species shown.

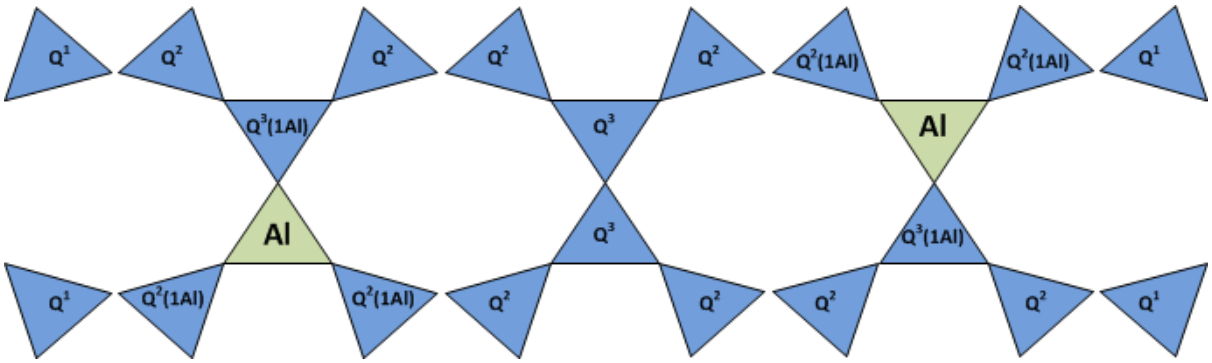

Site type						
Q^0	Q^1(1Al)	Q^1	Q^2(1Al)	Q^2	Q^3(1Al)	Q^3
0.00	0.00	0.18	0.18	0.36	0.09	0.09

Figure S1. Top: crosslinked C-(N)-A-S-H with MCL = 22. Bottom: distribution of silicon environments in the crosslinked C-(N)-A-S-H species. Silicate and aluminate tetrahedra are represented by blue and green triangles respectively.

The MCL and Al/Si values calculated by eqs.(7-8) using the values presented in Figure S1 are 22 and 0.1 respectively, in agreement with the actual MCL and Al/Si ratio of the structure.

Appendix B. Derivation of the Ca/Si and Ca/(Al+Si) ratios for a C-(N)-A-S-H gel represented by 9Å, anomalous 11Å, normal 11Å and 14Å tobermorites

Representation of the C-(N)-A-S-H phase by a mixture of 9Å, anomalous 11Å, normal 11Å and 14Å tobermorite species in the CSTM leads to Ca/Si and Ca/(Al+Si) ratios different from those presented in eqs.(34, 35). The tobermorites are represented by fractional contributions of silicon and aluminum to derive these relationships, leading to the following expressions for the total amounts of calcium and silicon in the C-(N)-A-S-H gel:

$$\begin{aligned}\left(Si\right)_{C-(N)-A-S-H} = {} & (Al+Si)_{14\mathring{A}}\, Si^{cf}_{14\mathring{A}} + \\ & (Al+Si)_{a11\mathring{A}}\, Si^{cf}_{a11\mathring{A}} + (Al+Si)_{n11\mathring{A}}\, Si^{cf}_{n11\mathring{A}} + (Al+Si)_{9\mathring{A}}\, Si^{cf}_{9\mathring{A}}\end{aligned} \tag{S1}$$

$$\begin{aligned}\left(Ca\right)_{C-(N)-A-S-H} = {} & (Al+Si)_{14\mathring{A}}\, Si^{cf}_{14\mathring{A}} (Ca/Si)_{14\mathring{A}} + (Al+Si)_{a11\mathring{A}}\, Si^{cf}_{a11\mathring{A}} (Ca/Si)_{a11\mathring{A}} + \\ & (Al+Si)_{n11\mathring{A}}\, Si^{cf}_{n11\mathring{A}} (Ca/Si)_{n11\mathring{A}} + (Al+Si)_{9\mathring{A}}\, Si^{cf}_{9\mathring{A}} (Ca/Si)_{9\mathring{A}}\end{aligned} \tag{S2}$$

where the subscripts $14\mathring{A}$, $a11\mathring{A}$, $n11\mathring{A}$ and $9\mathring{A}$ denote 14Å tobermorite, anomalous and normal 11Å tobermorite, and 9Å tobermorite respectively. The superscript cf is an abbreviation for chain fraction, describing the fractional contribution of each species to the chemistry of the aluminosilicate chain of the respective tobermorite species i.e. $Al/Si = (1-Si)/Si$. As the Al/Si ratio relationship is the same for non-crosslinked and crosslinked tobermorite species, it is possible to write:

$$(Al/Si)_{a11\mathring{A}} = (Al/Si)_{n11\mathring{A}} = (Al/Si)_{[C]} \tag{S3}$$

$$(Al/Si)_{14\mathring{A}} = (Al/Si)_{9\mathring{A}} = (Al/Si)_{[NC]} \tag{S4}$$

Thus, in terms of chain fraction:

58 $$(Si)^{cf}_{a11\mathring{A}} = (Si)^{cf}_{n11\mathring{A}} = (Si)^{cf}_{[C]} \quad \text{(S5)}$$

59 $$(Si)^{cf}_{14\mathring{A}} = (Si)^{cf}_{9\mathring{A}} = (Si)^{cf}_{[NC]} \quad \text{(S6)}$$

60 And

61 $$(Al)^{cf}_{a11\mathring{A}} = (Al)^{cf}_{n11\mathring{A}} = (Al)^{cf}_{[C]} \quad \text{(S7)}$$

62 $$(Al)^{cf}_{14\mathring{A}} = (Al)^{cf}_{9\mathring{A}} = (Al)^{cf}_{[NC]} \quad \text{(S8)}$$

63 Hence eqs.(S1, S2) can be re-written as:

64 $$(Si)_{C-(N)-A-S-H} = Si^{cf}_{[NC]}\left[(Al+Si)_{14\mathring{A}} + (Al+Si)_{9\mathring{A}}\right] + Si^{cf}_{[C]}\left[(Al+Si)_{a11\mathring{A}} + (Al+Si)_{n11\mathring{A}}\right] \quad \text{(S9)}$$

65 $$(Ca)_{C-(N)-A-S-H} = Si^{cf}_{[NC]}\left[(Al+Si)_{14\mathring{A}}(Ca/Si)_{14\mathring{A}} + (Al+Si)_{9\mathring{A}}(Ca/Si)_{9\mathring{A}}\right] + Si^{cf}_{[C]}\left[(Al+Si)_{a11\mathring{A}}(Ca/Si)_{a11\mathring{A}} + (Al+Si)_{n11\mathring{A}}(Ca/Si)_{n11\mathring{A}}\right] \quad \text{(S10)}$$

66 This leads to the formula for the overall Ca/Si ratio of the C-(N)-A-S-H gel:

67 $$(Ca/Si)_{C-(N)-A-S-H} = \frac{Si^{cf}_{[NC]}\left[(Al+Si)_{14\mathring{A}}(Ca/Si)_{14\mathring{A}} + (Al+Si)_{9\mathring{A}}(Ca/Si)_{9\mathring{A}}\right] + Si^{cf}_{[C]}\left[(Al+Si)_{a11\mathring{A}}(Ca/Si)_{a11\mathring{A}} + (Al+Si)_{n11\mathring{A}}(Ca/Si)_{n11\mathring{A}}\right]}{Si^{cf}_{[NC]}\left[(Al+Si)_{14\mathring{A}} + (Al+Si)_{9\mathring{A}}\right] + Si^{cf}_{[C]}\left[(Al+Si)_{a11\mathring{A}} + (Al+Si)_{n11\mathring{A}}\right]} \quad \text{(S11)}$$

68 By writing the chain fraction species in terms of Al/Si ratios we obtain:

$$\left(Ca/Si\right)_{C-(N)-A-S-H} = \left[\frac{(Al+Si)_{14\text{Å}}(Ca/Si)_{14\text{Å}} + (Al+Si)_{9\text{Å}}(Ca/Si)_{9\text{Å}}}{\left(1+\left(Al/Si\right)_{[NC]}\right)}\right] + \left[\frac{(Al+Si)_{a11\text{Å}}(Ca/Si)_{a11\text{Å}} + (Al+Si)_{n11\text{Å}}(Ca/Si)_{n11\text{Å}}}{\left(1+\left(Al/Si\right)_{[C]}\right)}\right] \Bigg/ \left[\frac{(Al+Si)_{14\text{Å}} + (Al+Si)_{9\text{Å}}}{\left(1+\left(Al/Si\right)_{[NC]}\right)}\right] + \left[\frac{(Al+Si)_{a11\text{Å}} + (Al+Si)_{n11\text{Å}}}{\left(1+\left(Al/Si\right)_{[C]}\right)}\right] \quad \text{(S12)}$$

This procedure can be similarly applied to derive the Ca/(Al+Si) ratio, which is:

$$Ca/(Al+Si)_{C-(N)-A-S-H} = \left[\frac{MCL_{14\text{Å}}(Ca/Si)_{14\text{Å}} + MCL_{9\text{Å}}(Ca/Si)_{9\text{Å}}}{\left(1+\left(Al/Si\right)_{[NC]}\right)}\right] + \left[\frac{MCL_{a11\text{Å}}(Ca/Si)_{a11\text{Å}} + MCL_{n11\text{Å}}(Ca/Si)_{n11\text{Å}}}{\left(1+\left(Al/Si\right)_{[C]}\right)}\right] \Bigg/ \left(MCL_{14\text{Å}} + MCL_{9\text{Å}} + MCL_{a11\text{Å}} + MCL_{n11\text{Å}}\right) \quad \text{(S13)}$$

Eqs.(S12, S13) reduce to eqs.(34, 35) if the C-(N)-A-S-H product is modeled as only one type of crosslinked and one type of non-crosslinked tobermorite species.

Appendix C. Analytical details, deconvolution procedures and deconvoluted ^{27}Al and ^{29}Si MAS NMR spectra

The composition of the slag used in the experimental work reported here is given in Table S1. All samples were activated with sodium metasilicate, added at a ratio of 8g Na_2SiO_3/100g GBFS, and had a water/binder ratio of 0.40. Samples were cured at 23°C in sealed molds, and demolded for manual crushing immediately before analysis.

Table S1. Oxide composition of the GBFS used in this work as determined by X-ray fluorescence. LOI is loss on ignition at 1000°C.

Component	(mass % as oxide)
SiO_2	33.8
Al_2O_3	13.7
Fe_2O_3	0.4
CaO	42.6
MgO	5.3
Na_2O	0.1
K_2O	0.4
Others	1.9
LOI	1.8
Specific gravity (kg/m^3)	2800
Blaine fineness (m^2/kg)	410
Average particle size (µm)	15

ESEM-EDS

Environmental scanning electron microscopy (ESEM) of alkali silicate-activated pastes after 7, 28 and 56 days of curing was conducted using an FEI Quanta instrument with a 15 kV accelerating voltage and a working distance of 10 mm. Polished samples were evaluated in low vacuum mode, using a backscatter detector, to avoid the need to coat the samples. A Link-Isis (Oxford Instruments) X-ray energy dispersive (EDS) detector was used to determine chemical compositions. An average of approximately 30 data points were collected for elemental analysis at each time of curing.

^{29}Si MAS NMR

Solid-state ^{29}Si MAS NMR spectra were collected at 119.1 MHz on a Varian VNMRS-600 (14.1 T) spectrometer using a probe for 4 mm o.d. zirconia (PSZ) rotors and a spinning speed of 10.0 kHz. The ^{29}Si MAS experiments employed a pulse width of 4 μs, a relaxation delay of 20 s and 4096 scans. Solid-state ^{27}Al MAS NMR spectra were acquired at 156.3 MHz on the same instrument, with a pulse width of 0.5 μs, a relaxation delay of 2 s, and at least 1000 scans. All spectra were collected with a pulse angle of 51°. ^{29}Si and ^{27}Al chemical shifts are referenced to external samples of tetramethylsilane (TMS) and a 1.0 M aqueous solution of $AlCl_3.6H_2O$, respectively.

Deconvolution of the ^{29}Si MAS NMR spectra was performed using the minimum possible number of component peaks to describe the spectrum accurately. The spectra were fitted with Gaussian functions with the specified full width at half height (FWHH) always <10 ppm, which were assigned to connectivity states based on information available in the literature for cements,[20,41,59] for aluminosilicate zeolite systems,[60] and for silicate-activated slag binders.[24] Peak positions and widths were held constant throughout all spectral deconvolutions. The component peaks assigned to the remnant anhydrous slag were rescaled by a single factor in each spectrum to provide the appropriate lineshape in the region of the spectra where the contribution of the anhydrous slag is expected. This method was chosen as it was shown in a recent study [49] that quantification of ^{29}Si MAS NMR spectra of AAS cements and blended cements containing slag were most appropriately described in this way, enabling the extent of reaction of the remnant anhydrous slag component to be calculated directly.

Assignment of the peak located at a chemical shift of -93 ppm to Q^4(3Al) species is justified because this is the only plausible assignment consistent with a mixed crosslinked/non-crosslinked

tobermorite-like C-(N)-A-S-H type gel for the spectral deconvolution results determined in this work. The only possible alternative silicate coordination environment that is located at approximately -93 ppm and is consistent with the established nature of AAS binder are Q^3 units,[60] which are found in the crosslinked tobermorite-like structures that are expected in the C-(N)-A-S-H type gel. Hypothetical deconvolution of the ^{29}Si MAS NMR spectra to exclusively assign the peak at -93 ppm to Q^3 units yields the results shown in Table S2.

Table S2. Summary of hypothetical Q^n environments in ^{29}Si MAS NMR spectra of alkali-activated slag pastes as a function of the time of curing given that the assignment of the peak located at a chemical shift of -93 ppm corresponds exclusively to Q^3 units. Estimated uncertainty in site percentages is ± 1%, based on the influence of the signal/noise ratio of the spectra on the deconvolution procedures.

age	unreacted slag	reaction products						
		Q^0	Q^1(I)	Q^1(II)	Q^2(1Al)	Q^2	Q^3(1Al)	Q^3
		-74 ppm	-78 ppm	-80 ppm	-83 ppm	-86 ppm	-89 ppm	-93 ppm
unreacted	100	-	-	-	-	-	-	-
7 days	39	4	14	11	18	11	4	-
28 days	24	7	18	13	22	12	5	-
56 days	21	10	18	11	19	13	7	1

It is readily observed in Table S2 that the hypothetical spectral deconvolution for the 56 days sample is inconsistent with the structural definition of the C-(N)-A-S-H type gel as a mixture of crosslinked and non-crosslinked structures, as described by the structural constraints of the CSTM (Figure 3). This is because there are not enough Q^2 units to account for the amount of Q^3(1Al) and Q^3 species identified in the hypothetical deconvolution for the 56 days sample (Table C2), i.e. $2(Q^3(1Al)+Q^3) > Q^2$, given this structural definition of the C-(N)-A-S-H type gel. Therefore, given that the assignment of Q^3 species does not agree with the established nature of the AAS binder, the only remaining possibility is to attribute the peak located at -93 ppm to Q^4(3Al) species.

As discussed in the body of the article, inclusion of Q^4(3Al) species necessitates the presence of another four-connected silicate species in the experimental ^{29}Si MAS NMR spectra. Here it is assumed that the only Q^4 type silicate units in the samples studied were Q^4(4Al) and Q^4(3Al), which is consistent with the chemistry of Al-rich metakaolin-based geopolymers observed in MAS NMR [51] and predicted by a statistical thermodynamic model.[50] Quantification of the Q^4(4Al) component in the ^{29}Si MAS NMR spectral deconvolutions was performed using eq.(S14) assuming that the Q^4 type units are present in an addition Al-rich phase separate from the C-(N)-A-S-H type gel:

$$I^{*}_{Q^4(4Al)} = I_{Q^4(3Al)}\left[\frac{\frac{3}{5}\left(Si/Al\right)^{*}-1}{1-\left(Si/Al\right)^{*}}\right] \quad \text{(S14)}$$

where $I_{Q^4(3Al)}$ is the relative intensity of the Q^4(3Al) component determined from deconvolution of the experimental ^{29}Si MAS NMR spectra, $I^{*}_{Q^4(4Al)}$ is the calculated relative intensity of Q^4(4Al) components and $\left(Si/Al\right)^{*}$ is the assumed Si/Al ratio for the Q^4-containing additional phase. An Si/Al ratio of 1.2 was used here, which is consistent with the composition of aluminosilicate geopolymer gels determined from MAS NMR [51] and statistical thermodynamic model predictions.[50] Inclusion of Q^4 type silicate units in the analysis is also consistent with the ^{27}Al MAS NMR spectra shown in this work, which contain significant levels of intensity in the four-connected Al[4] region at between approximately 52-62 ppm.[60]

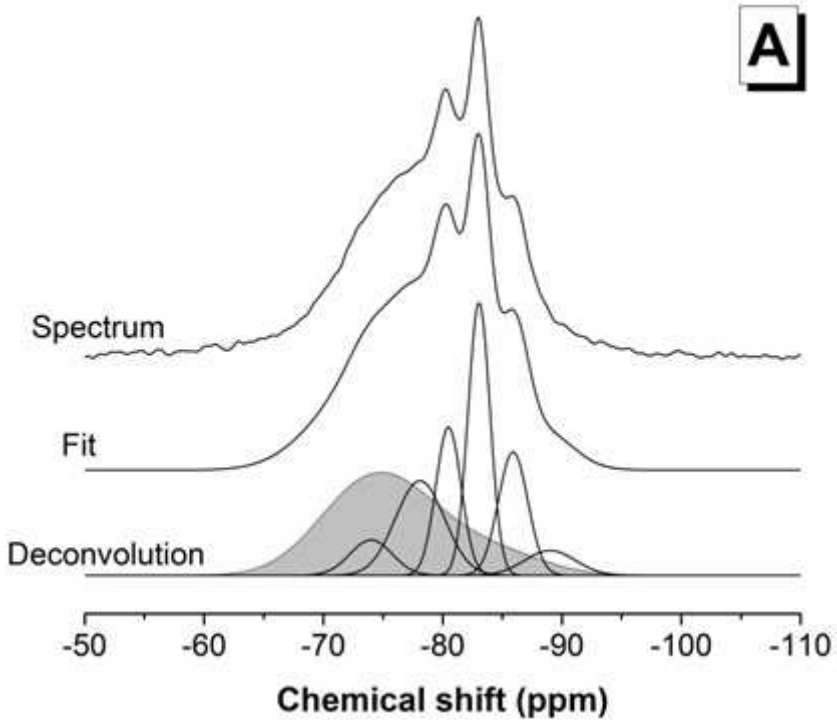
A
Spectrum
Fit
Deconvolution
-50
-60
-70
-80
-90
-100
-110
Chemical shift (ppm)

159

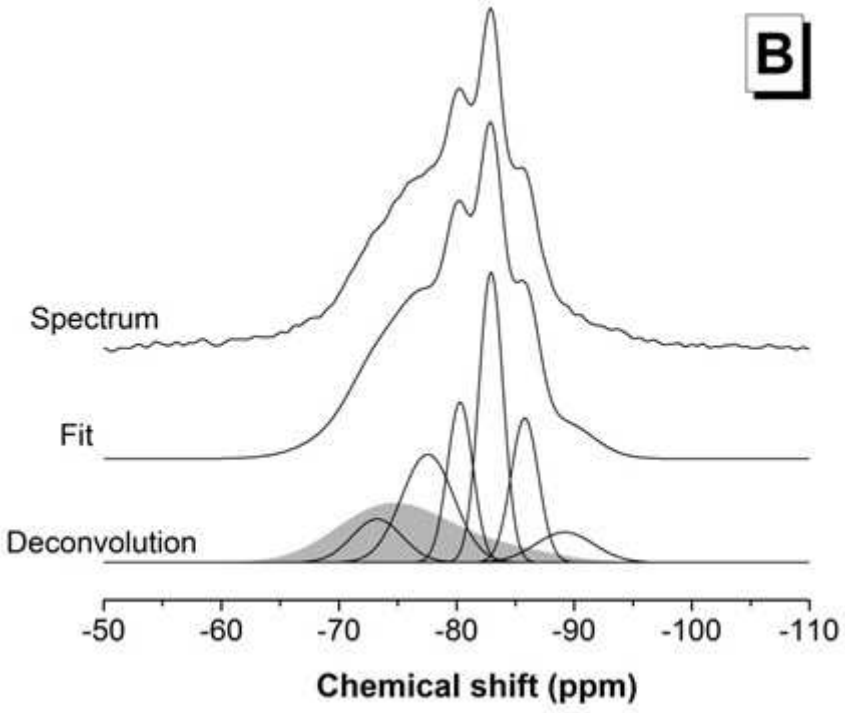
B
Spectrum
Fit
Deconvolution
-50
-60
-70
-80
-90
-100
-110
Chemical shift (ppm)

160

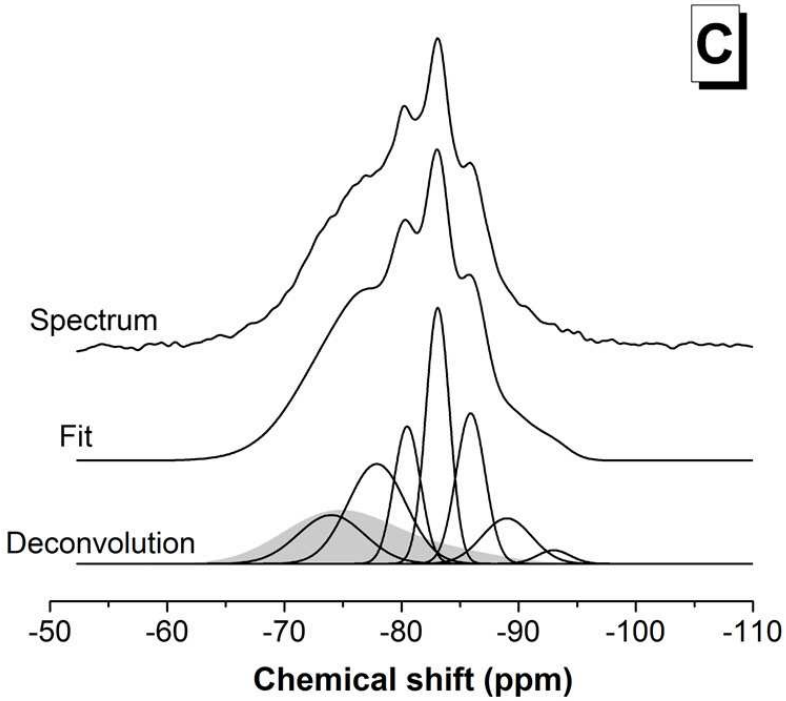

Figure S2. Deconvoluted ^{29}Si MAS NMR spectra (14.1 T, ν_R=10 kHz) of sodium silicate-activated slag cured for (A) 7days, (B) 28 days and (C) 56 days. The dark gray band represents the contribution of the remnant anhydrous slag

^{27}Al MAS NMR

^{27}Al MAS NMR spectra were deconvoluted using the Dmfit software [61] and included consideration of the effects of quadrupolar coupling on the component peak shapes. The secondary reaction products formed in the sodium silicate activated slag binder and taken into account in the ^{27}Al MAS NMR spectral deconvolutions were also identified through X-ray diffraction.[24,42] Component peaks were matched to coordination and connectivity states that are consistent with the assignation of these sites in the available cement literature.[12,22,38,62,63,64] Quadrupolar coupling parameters used to define the component peaks of these secondary products in the deconvolutions were taken from the literature (Table S3). The component peaks of the remnant anhydrous slag and C-(N)-A-S-H product were defined using quadrupolar coupling parameters that provided a good fit to the experimental spectra and were consistent with the established values for zeolites. The remnant anhydrous slag component peaks were rescaled by a single factor assuming congruent dissolution of

the slag precursor, as calculated from the ^{29}Si MAS NMR spectral deconvolutions. Peak positions were held constant and simulated line-broadening was applied in Dmfit to match the experimental spectra throughout the deconvolution process.

Table S3. The phases and associated quadrupolar coupling parameters used in the ^{27}Al MAS NMR spectral deconvolutions

assignment	unreacted slag	q^2(I)	q^2(II)	q^3	$Al^{[5]}$	AFm	HT	HT/TAH	TAH
C_q (MHz)	5.93	1.97	3.40	4.13	4.00	1.80	1.55	3.55	1.25
reference	65*	65*	65*	65*	65*	64	63	63	22

* consistent with the quadrupolar coupling parameters reported for the aluminosilicate species in the referenced paper

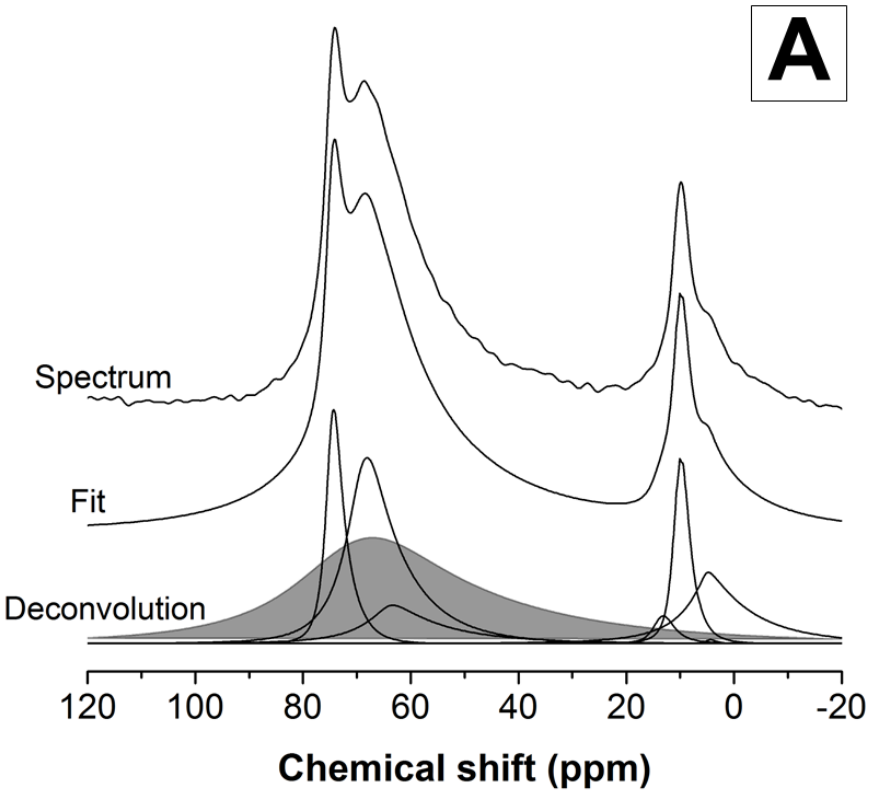
A
Spectrum
Fit
Deconvolution
120
100
80
60
40
20
0
-20
Chemical shift (ppm)

189

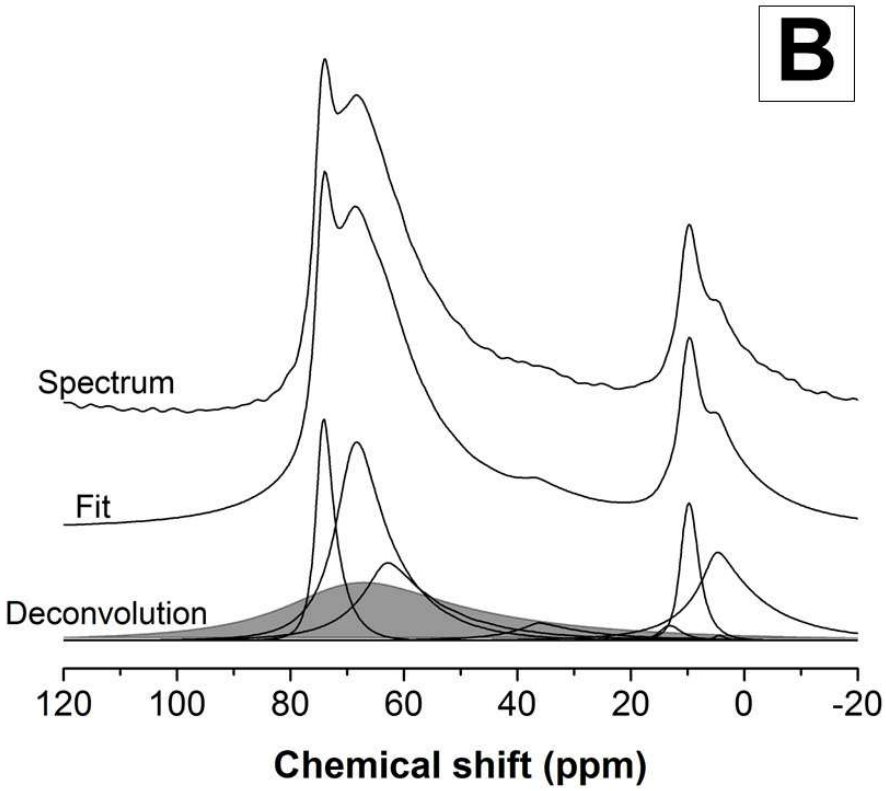
B
Spectrum
Fit
Deconvolution
120
100
80
60
40
20
0
-20
Chemical shift (ppm)

190

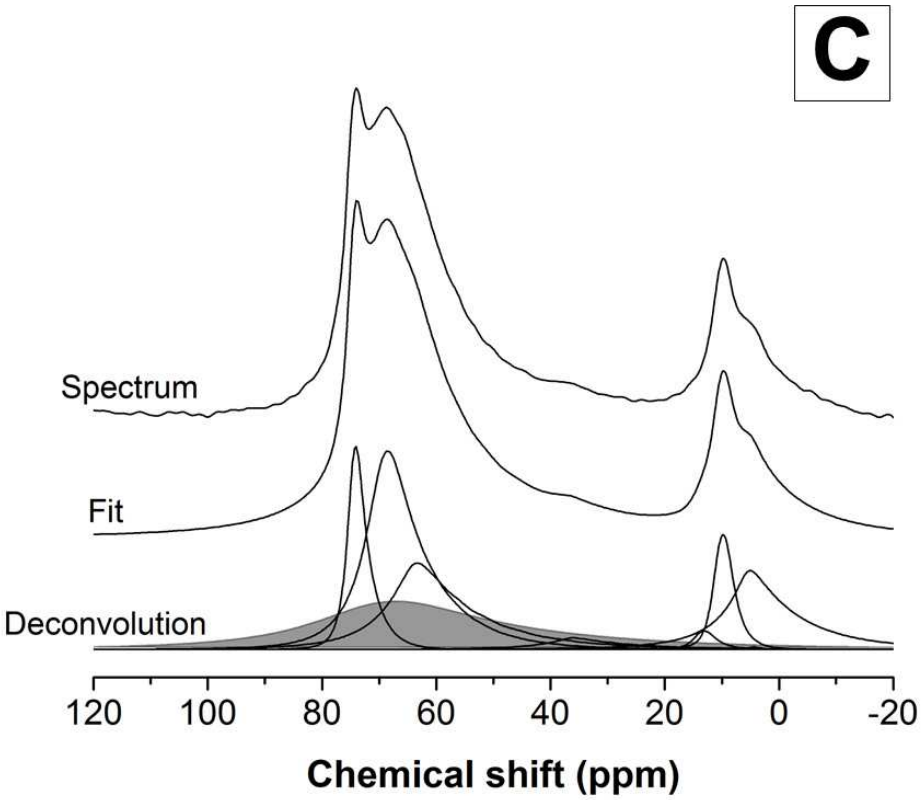

Figure S3. Deconvoluted ^{27}Al MAS NMR spectra (14.1 T, ν_R=10 kHz) of alkali-activated slag cured for (A) 7days, (B) 28 days and (C) 56 days. The dark grey band represents the contribution of the remnant anhydrous slag.

References

(refs. 1-58 are listed in the body of the article)

(59) Barnes, J. R.; Clague, A. D. H.; Clayden, N. J.; Dobson, C. M.; Hayes, C. J.; Groves, G. W.; Rodger, S. A., Hydration of Portland cement followed ^{29}Si solid-state NMR spectroscopy. *J. Mater. Sci. Lett.* **1985**, *4*, 1293-1295.

(60) Engelhardt, G.; Michel, D., *High-Resolution Solid-State NMR of Silicates and Zeolites*. John Wiley & Sons: Chichester, 1987; p 485.

(61) Massiot, D.; Fayon, F.; Capron, M.; King, I.; Le Calvé, S.; Alonso, B.; Durand, J.-O.; Bujoli, B.; Gan, Z.; Hoatson, G., Modelling one- and two-dimensional solid-state NMR spectra. *Magn. Reson. Chem.* **2002**, *40*, 70-76.

(62) MacKenzie, K. J. D.; Meinhold, R. H.; Sherrif, B. L.; Xu, Z., ^{27}Al and ^{25}Mg solid-state magic-angle spinning nuclear magnetic resonance study of hydrotalcite and its thermal decomposition sequence. *J. Mater. Chem.* **1993**, *3*, 1263-1269.

(63) Sideris, P. J.; Blanc, F.; Gan, Z.; Grey, C. P., Identification of Cation Clustering in Mg–Al Layered Double Hydroxides Using Multinuclear Solid State Nuclear Magnetic Resonance Spectroscopy. *Chem. Mater.* **2012**, *24*, 2449-2461.

(64) Skibsted, J.; Henderson, E.; Jakobsen, H. J., Characterization of calcium aluminate phases in cements by aluminum-27 MAS NMR spectroscopy. *Inorg. Chem.* **1993**, *32*, 1013-1027.

(65) Klinowski, J., Nuclear magnetic resonance studies of zeolites. *Prog. Nucl. Magn. Reson. Spectr.* **1984**, *16*, 237-309.